

## Electrochemical Evaluation and DFT Studies of 2-(4-chlorophenyl)-3-hydroxy-4,6-dioxo-8-phenyl-4,6-dihydropyrimido[2,1-b][1,3]thiazine-7-carbonitrile of Carbon Steel Corrosion in Hydrochloric Acid

M. Belayachi<sup>1</sup>, H. Serrar<sup>2</sup>, A. El Assyry<sup>3</sup>, H. Oudda<sup>1</sup>, S. Boukhris<sup>2</sup>, M. Ebn Touhami<sup>4</sup>, A. Zarrouk<sup>5,\*</sup>, B. Hammouti<sup>5,6</sup>, Eno E. Ebenso<sup>7,\*</sup>, A. El Midaoui<sup>1</sup>

<sup>1</sup> Laboratoire des procédés de séparation, Faculté des Sciences, Université Ibn Tofail, Kenitra, BP 133, Kenitra, Morocco.

<sup>2</sup> Laboratoire de Synthèse Organique, Organométallique et Théorique, Faculté des Sciences, Université Ibn Tofail, BP 133, Kenitra, Morocco.

<sup>3</sup> Laboratoire d'Optoélectronique et de Physico-chimie des Matériaux (Unité associée au CNRST), Département de Physique, Université Ibn Tofail, B.P. 133, Kénitra, Maroc.

<sup>4</sup> Laboratoire Matériaux, Electrochimie et Environnement, Faculté des Sciences, Université Ibn Tofail, kenitra, Morocco.

<sup>5</sup> LCAE-URAC18, Faculté des Sciences, Université Mohammed 1<sup>er</sup>, Oujda, Morocco.

<sup>6</sup> Petrochemical Research Chair, Chemistry Department, College of Science, King Saud University, P.O. Box 2455, Riyadh 11451, Saudi Arabia.

<sup>7</sup> Material Science Innovation & Modelling (MaSIM) Research Focus Area, Faculty of Agriculture, Science and Technology, North-West University (Mafikeng Campus), Private Bag X2046, Mmabatho 2735, South Africa

\*E-mail: [azarrouk@gmail.com](mailto:azarrouk@gmail.com), [Eno.Ebenso@nwu.ac.za](mailto:Eno.Ebenso@nwu.ac.za)

Received: 15 November 2014 / Accepted: 29 January 2015 / Published: 24 February 2015

In present study corrosion inhibition property of 2-(4-chlorophenyl)-3-hydroxy-4,6-dioxo-8-phenyl-4,6-dihydropyrimido[2,1-b][1,3]thiazine-7-carbonitrile (CHPPC) in 1.0 M HCl was investigated using electrochemical impedance spectroscopy, potentiodynamic polarization and DFT studies. From electrochemical measurements it is observed that inhibition efficiency increases with CHPPC concentration and maximum efficiency (98.9) was obtained at 1.0 mM. The potentiodynamic study reveals that pyrimidothiazine derivative is a mixed type inhibitor with predominant cathodic action. EIS plot indicates that the addition of inhibitor increases the charge-transfer resistance ( $R_{ct}$ ) and decreases the double-layer capacitance ( $C_{dl}$ ) of the corrosion process, these observation reveal that investigated pyrimidothiazine derivative inhibits carbon steel corrosion by adsorption mechanism. Adsorption of pyrimidothiazine derivative on carbon steel surface obeys the Langmuir adsorption isotherm. The effect of temperature on the corrosion rate was investigated and some thermodynamic parameters were also calculated in order to explain the mechanism of adsorption. A theoretical study

of the corrosion inhibition efficiency of this pyrimidothiazine derivative, was carried out using density functional theory (DFT) at the B3LYP/6-31G(d) level of theory.

**Keywords:** Pyrimidothiazine derivative, Steel, Corrosion inhibition, Electrochemical techniques, DFT

## 1. INTRODUCTION

The use of corrosion inhibitors is an effective and economic method for controlling corrosion of metals and alloys in many industrial processes during pickling processes, industrial acid cleaning, oil and gas well acidizing [1]. Organic compounds containing nitrogen, sulphur, oxygen atoms and multiple bonds act as effective corrosion inhibitors and inhibit corrosion by adsorption mechanism [2-23].

It is generally accepted that the primary step in the protecting action of an inhibitor in the acid metal corrosion is adsorption of the organic molecule onto the metal surface, which is usually oxide-free. The adsorption requires the existence of attractive forces between the metal surface (adsorbent) and the organic molecule (adsorbate). According to the type of forces, adsorption can be physisorption, chemisorptions or a combination of both [24,25]. Physisorption is weak undirected interaction and is due to electrostatic attraction between inhibiting organic ions or dipoles and the electrically charged surface of metal. A peculiarity of physisorption is that the ions or dipoles are non in direct physical contact with the metal. A layer of water molecules separates the metal from the ions or dipoles. Physisorption involves rapid interaction between adsorbent and adsorbate but it is also easily removed from surface with the temperature increase.

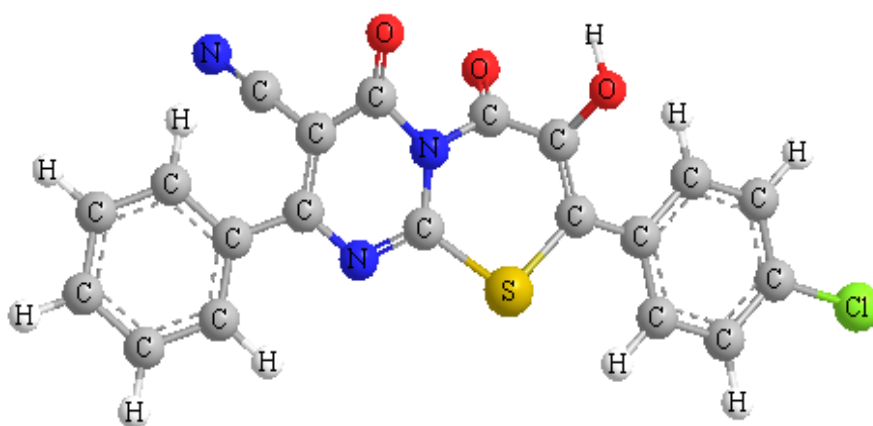


**Figure 1.** The chemical structure of the studied pyrimidothiazine derivative.

Hence, in the present study 2-(4-chlorophenyl)-3-hydroxy-4,6-dioxo-8-phenyl-4,6-dihydropyrimido[2,1-b][1,3]thiazine-7-carbonitrile (CHPPC), is selected. The choice of this compound was based on the consideration that this compound contains many  $\pi$ -electrons and hetero atoms which induce greater adsorption of the inhibitor compared with other compounds organic. By considering the

remarks mentioned above, in the present work, the inhibition effect of CHPPC on the corrosion of carbon steel in 1.0 M HCl solution at 303-333K was studied using potentiodynamic polarisation curves and electrochemical impedance spectroscopy (EIS) methods. Density functional theory used to calculate some quantum chemical parameters which will assist in the interpretation of inhibition process. The chemical structure of the studied pyrimidothiazine derivative is given in Fig 1.

## 2. EXPERIMENTAL METHODS

### 2.1. Materials

The steel used in this study is a carbon steel (CS) (Euronorm: C35E carbon steel and US specification: SAE 1035) with a chemical composition (in wt%) of 0.370 % C, 0.230 % Si, 0.680 % Mn, 0.016 % S, 0.077 % Cr, 0.011 % Ti, 0.059 % Ni, 0.009 % Co, 0.160 % Cu and the remainder iron (Fe).

### 2.2. Solutions

The aggressive solutions of 1.0 M HCl were prepared by dilution of analytical grade 37% HCl with distilled water. The concentration range of 2-(4-chlorophenyl)-3-hydroxy-4,6-dioxo-8-phenyl-4,6-dihydropyrimido[2,1-b][1,3]thiazine-7-carbonitrile (CHPPC) used was  $10^{-6}$  M to  $10^{-3}$  M.

### 2.3. Polarization measurements

#### 2.3.1. Electrochemical impedance spectroscopy

The electrochemical measurements were carried out using Volta lab (Tacussel- Radiometer PGZ 100) potentiostat and controlled by Tacussel corrosion analysis software model (Voltmaster 4) at under static condition. The corrosion cell used had three electrodes. The reference electrode was a saturated calomel electrode (SCE). A platinum electrode was used as auxiliary electrode of surface area of  $1 \text{ cm}^2$ . The working electrode was carbon steel. All potentials given in this study were referred to this reference electrode. The working electrode was immersed in test solution for 30 minutes to establish steady state open circuit potential ( $E_{ocp}$ ). After measuring the  $E_{ocp}$ , the electrochemical measurements were performed. All electrochemical tests have been performed in aerated solutions at 303 K. The EIS experiments were conducted in the frequency range with high limit of 100 kHz and different low limit 0.1 Hz at open circuit potential, with 10 points per decade, at the rest potential, after 30 min of acid immersion, by applying 10 mV ac voltage peak-to-peak. Nyquist plots were made from these experiments. The best semicircle can be fit through the data points in the Nyquist plot using a non-linear least square fit so as to give the intersections with the  $x$ -axis.

The inhibition efficiency of the inhibitor was calculated from the charge transfer resistance values using the following equation:

$$\eta_z \% = \frac{R_{ct}^i - R_{ct}^{\circ}}{R_{ct}^i} \times 100 \quad (1)$$

where,  $R_{ct}^{\circ}$  and  $R_{ct}^i$  are the charge transfer resistance in absence and in presence of inhibitor, respectively.

### 2.3.2. Potentiodynamic polarization

The electrochemical behaviour of carbon steel sample in inhibited and uninhibited solution was studied by recording anodic and cathodic potentiodynamic polarization curves. Measurements were performed in the 1.0 M HCl solution containing different concentrations of the tested inhibitor by changing the electrode potential automatically from -800 to -100 mV versus corrosion potential at a scan rate of 2 mV s<sup>-1</sup>. The linear Tafel segments of anodic and cathodic curves were extrapolated to corrosion potential to obtain corrosion current densities ( $I_{corr}$ ). From the polarization curves obtained, the corrosion current ( $I_{corr}$ ) was calculated by curve fitting using the equation:

$$I = I_{corr} \left[ \exp\left(\frac{2.3\Delta E}{\beta_a}\right) - \exp\left(\frac{2.3\Delta E}{\beta_c}\right) \right] \quad (2)$$

The inhibition efficiency was evaluated from the measured  $I_{corr}$  values using the relationship:

$$\eta_{IE} \% = \frac{I_{corr} - I_{corr(i)}}{I_{corr}} \times 100 \quad (3)$$

where,  $I_{corr}$  and  $I_{corr(i)}$  are the corrosion current density in absence and presence of inhibitor, respectively.

### 2.4. Computational procedures

Density Functional theory (DFT) has been recently used [26-29] to describe the interaction between the inhibitor molecule and the surface as well as the properties of these inhibitors concerning their reactivity. The molecular band gap was computed as the first vertical electronic excitation energy from the ground state using the time-dependent density functional theory (TD-DFT) approach as implemented in Gaussian 03 [30]. For these seek, some molecular descriptors, such as HOMO and LUMO energy values, frontier orbital energy gap, molecular dipole moment, electronegativity ( $\chi$ ), global hardness ( $\eta$ ), softness(S), the fraction of electron transferred ( $\Delta N$ ), were calculated using the DFT method and have been used to understand the properties and activity of the newly prepared compounds and to help in the explanation of the experimental data obtained for the corrosion process.

According to Koopman's theorem [31] the ionization potential (IE) and electron affinity (EA) of the inhibitors are calculated using the following equations.

$$I = -E_{HOMO} \quad (4)$$

$$E = -E_{LUMO} \quad (5)$$

Thus, the values of the electronegativity ( $\chi$ ) and the chemical hardness ( $\eta$ ) according to Pearson, operational and approximate definitions can be evaluated using the following relations [32]:

$$\chi = \frac{IE + EA}{2} \quad (6)$$

$$\eta = \frac{IE - EA}{2} \quad (7)$$

The number of transferred electrons ( $\Delta N$ ) was also calculated depending on the quantum chemical method [33,34] by using the equation;

$$\Delta N = \frac{\chi_{Fe} - \chi_{inh}}{2(\eta_{Fe} + \eta_{inh})} \quad (8)$$

Where  $\chi_{Fe}$  and  $\chi_{inh}$  denote the absolute electronegativity of iron and inhibitor molecule  $\eta_{Fe}$  and  $\eta_{inh}$  denote the absolute hardness of iron and the inhibitor molecule respectively. In this study, we use the theoretical value of  $\chi_{Fe} = 7.0 \text{ eV mol}^{-1}$  and  $\eta_{Fe} = 0 \text{ eV mol}^{-1}$ , for calculating the number of electron transferred.

### 3. RESULTS AND DISCUSSION

#### 3.1. Polarization curves

Fig. 2 shows Tafel polarization curves of carbon steel in hydrochloric acid in the absence and presence of different concentrations of CHPPC at 303 K. The associated corrosion parameters such as  $E_{corr}$ , cathodic Tafel slopes ( $\beta_c$ ) and corrosion current density ( $I_{corr}$ ) are listed in Table 1.

It is clear that the addition of CHPPC causes a decrease in the corrosion rate, i.e. shifts the cathodic and anodic curves to lower values of current densities. Namely, both cathodic and anodic reactions of carbon steel electrode corrosion are inhibited by the inhibitor in acidic medium. This may be ascribed to adsorption of inhibitor over the corroded surface of carbon steel [35]. It follows from the data of Table 1 that the corrosion current,  $I_{corr}$  decreases, while  $\eta_{IE}\%$  enhances with increase in inhibitor concentration. The decrease in the corrosion current density was observed for the CHPPC, corresponding to a maximum efficiency of 98.9% at  $1 \times 10^{-3} \text{ M}$ .

Further inspection of Table 1 reveals that the presence of CHPPC does not remarkably shift the  $E_{corr}$ , therefore, the selected compound can be described as mixed-type inhibitor with predominant cathodic action for carbon steel corrosion in 1.0 M HCl, and the inhibition of the compound on carbon steel is caused by adsorption, namely, the inhibition effect results from the reduction of the reaction area on the surface of the carbon steel [36]. The value of  $\beta_c$  slight changed, indicates that the cathodic corrosion mechanism of steel does not change. As it is shown in Fig. 2, cathodic current-potential curves give rise to parallel Tafel lines, which indicate that oxygen reduction reaction is activation controlled and that the addition of the CHPPC does not modify the mechanism of this process [37]. The results demonstrate that the oxygen reduction is inhibited and that the inhibition efficiency increases with inhibitor concentration.

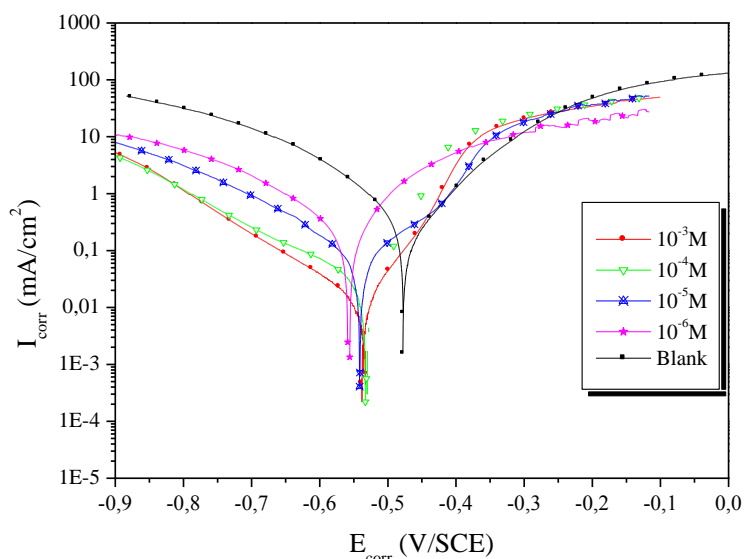


**Figure 2.** Polarisation curves of carbon steel in 1.0 M HCl for various concentrations of CHPPC.

**Table 1.** Polarization data of carbon steel in 1.0 M HCl without and with addition of inhibitor at 303 K.

Inhibitor	Conc (M)	$-E_{corr}$ (mV/SCE)	$-\beta_c$ (mV dec <sup>-1</sup> )	$I_{corr}$ ( $\mu\text{A cm}^{-2}$ )	$\eta_{IE}$ (%)
HCl	1.0	479	190	1070	-----
CHPPC	$10^{-3}$	531	151	11	98.9
	$10^{-4}$	532	154	21	98.0
	$10^{-5}$	526	176	112	89.5
	$10^{-6}$	558	159	268	74.9

### 3.2. Electrochemical impedance spectroscopy

#### 3.2.1. Effect of concentration inhibitor

Electrochemical impedance spectroscopy (EIS) is an effective method for corrosion studies of metallic materials. The effect of CHPPC concentration on the impedance spectra of carbon steel in 1.0 M HCl solutions at 303 K is recorded in Fig. 3 (Nyquist plots). It is clear to see that the impedance spectra are significantly changed with addition of different CHPPC concentration. From the Nyquist plots, it was also observed that, even the presence of CHPPC does not alter the style of impedance plots, thus indicating the addition of CHPPC does not change the mechanism for the dissolution of carbon steel in 1.0 M HCl solution [38-40].

The impedance diagrams show only one capacitive loop represented by slightly depressed semicircle which indicates that the corrosion of carbon steel in 1.0 M HCl solution is mainly controlled by charge transfer process and formation of a protective layer on the

carbon steel surface. The diameter of the capacitive loop increases with the increase of CHPPC concentration proposing that the formed inhibitive film was strengthened by the addition of CHPPC [41]. The depressed semicircles are generally attributed to the frequency dispersion as well as roughness and inhomogeneities of solid surface, and mass transport process [42], distribution of the active sites, adsorption of inhibitors [43-47].

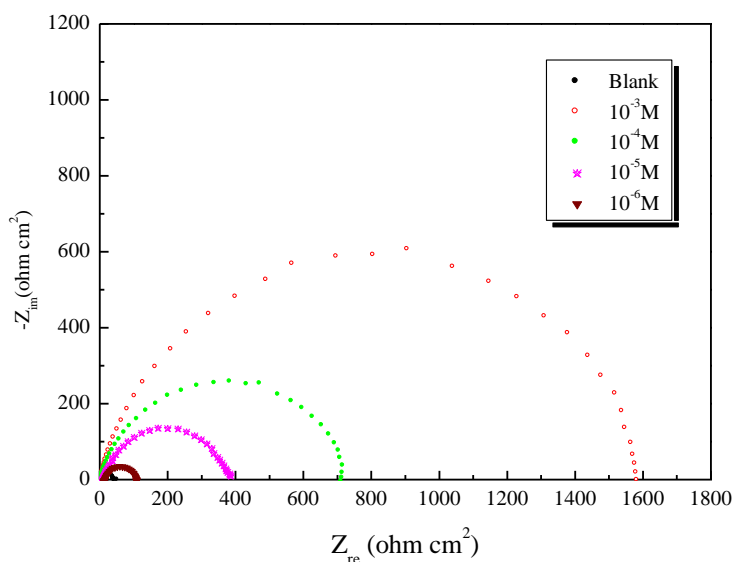


**Figure 3.** Nyquist diagrams for carbon steel in 1.0 M HCl containing different concentrations of CHPPC at 303 K.

The impedance parameters such as the double layer capacitance ( $C_{dl}$ ), the charge-transfer resistance ( $R_{ct}$ ) and the inhibition efficiency ( $\eta_z$  (%)) derived from Nyquist diagrams are given in Table 2.

**Table 2.** Impedance parameters for corrosion of steel in 1.0 M HCl in the absence and presence of different concentrations of CHPPC at 303 K.

Conc (M)	$R_{ct}$ ( $\Omega$ cm <sup>2</sup> )	$f_{max}$ (Hz)	$C_{dl}$ ( $\mu$ F/cm <sup>2</sup> )	$\eta_z$ (%)	$\theta$
Blank	42	39.2	96.7	---	---
$10^{-3}$	1660	4.8	20.0	97	0.97
$10^{-4}$	749	6.0	35.2	94	0.94
$10^{-5}$	394	6.0	66.3	89	0.89
$10^{-6}$	98	19.2	84.7	57	0.57

It was observed from the obtained EIS data that  $R_{ct}$  increases and  $C_{dl}$  decreases with the increasing of inhibitor concentrations. The increase in  $R_{ct}$  values, and consequently of inhibition efficiency, may be due to the gradual replacement of water molecules by the adsorption of the inhibitor molecules on the metal surface to form an adherent film on the metal surface, and this suggests that the coverage of the metal surface by the film decreases the double layer thickness. Also, this decrease of  $C_{dl}$  at the metal/solution interface with increasing the inhibitor concentration can result from a decrease in local dielectric constant which indicates that the inhibitor was adsorbed on the surface at both anodic and cathodic sites [48].

### 3.3.2. Effect of temperature

The effect of rising temperature on the corrosion current density of carbon steel in free in 1.0 M HCl solution containing 1.0 mM of 2-(4-chlorophenyl)-3-hydroxy-4,6-dioxo-8-phenyl-4,6-dihydropyrimido[2,1-b][1,3]thiazine-7-carbonitrile (CHPPC) was tested in the temperature range of 303-333 K using EIS measurements. Similar curves to Fig.3 were obtained (not shown).

The values of the electrochemical parameters obtained from Nyquist plots are given in Table 3.

**Table 3.** Various corrosion parameters for carbon steel in 1.0 M HCl in absence and presence of optimum concentration of CHPPC at different temperatures.

Temp (K)	$R_{ct}$ ( $\Omega\text{ cm}^2$ )	$C_{dl}$ ( $\mu\text{F cm}^2$ )	$\eta_z$ (%)
303	42	96.7	---
313	29	234	---
323	25	549	---
333	6	636	---
303	1660	20.0	97
313	387	34.3	92
323	195	56.2	91
333	74	314.3	87

Values of  $R_{ct}$  were employed to calculate values of the corrosion current density ( $I_{corr}$ ) at various temperatures in absence and presence of CTPTC using the following equation [49]:

$$I_{corr} = RT(zFR_{ct})^{-1} \quad (9)$$

where R is the universal gas constant ( $R = 8.314\text{ J mol}^{-1}\text{ K}^{-1}$ ), T is the absolute temperature, z is the valence of iron ( $z = 2$ ), F is the Faraday constant ( $F = 96\,485\text{ coulomb}$ ) and  $R_{ct}$  is the charge transfer resistance.

The activation energy of corrosion process can be obtained by investigating the influence of temperature on the corrosion and corrosion inhibition. Consequently some information about



adsorption mechanism of the inhibitor can be obtained from the activation energy values. A plot of  $\ln I_{corr}$  vs  $T^{-1}$  obeys Arrhenius equation [50]:

$$\ln(I_{corr}) = -\frac{E_a}{RT} + \text{constant} \quad (10)$$

EIS measurements were utilized to obtain the  $I_{corr}$  values using the equation (9) of carbon steel in the absence and presence of  $10^{-3}$  M of CHPPC at different temperatures of 303-333K. These values were plotted as shown in Fig. 4. The values of activation energy of corrosion were determined from the slope of  $\ln(I_{corr})$  versus  $1/T$  plots [51]. The  $E_a$  values for carbon steel in the absence and presence of  $10^{-3}$  M of CHPPC were calculated and listed in Table 4. The value of  $E_a$  found for CHPPC is higher than that obtained for 1.0 M HCl solution. The increase in the apparent activation energy may be interpreted as physical adsorption that occurs in the first stage [52]. Szauer and Brand explained that the increase in activation energy can be attributed to an appreciable decrease in the adsorption of the inhibitor on the carbon steel surface with increase in temperature.

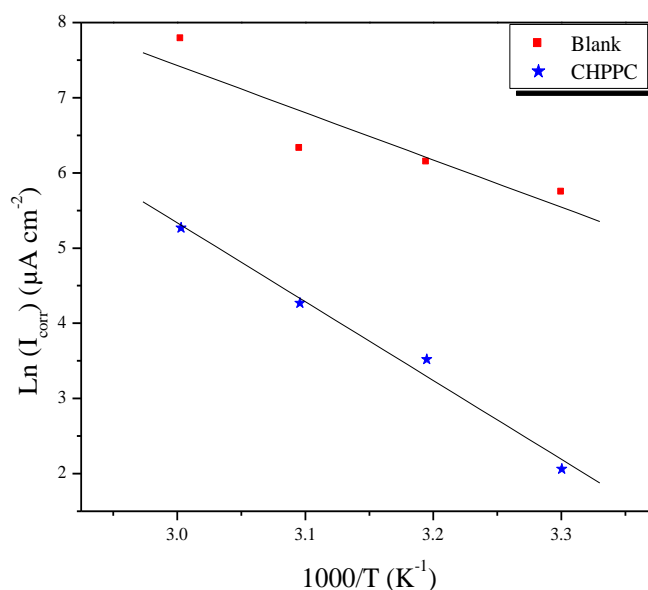


**Figure 4.** Arrhenius plots of carbon steel in 1.0 M HCl with and without  $10^{-3}$  M of CHPPC.

A transition state complex is decays to products after forming the high energy [53]. The mathematical form of transition state theory is shown as below:

$$I_{corr} = \frac{RT}{Nh} \exp\left(\frac{\Delta S_a}{R}\right) \exp\left(-\frac{\Delta H_a}{RT}\right) \quad (11)$$

where  $I_{corr}$  is the corrosion rate,  $A = RT/Nh$  is the pre-exponential factor,  $h$  is Planck's constant,  $N$  is the Avogadro number,  $R$  is the universal gas constant,  $\Delta H_a$  is the enthalpy of activation and  $\Delta S_a$  is the entropy of activation.

The values of enthalpy and entropy of activation for carbon steel corrosion in 1.0 M HCl in absence and presence of CHPPC can be evaluated from the slope and intercept of the curve of  $\ln(I_{corr}/T)$  versus  $1/T$ , respectively as shown in Fig. 5.

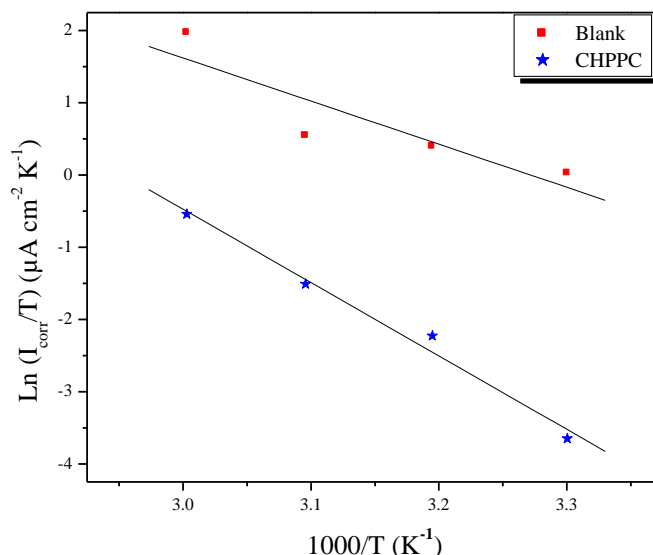


**Figure 5.** Relation between  $\text{Ln}(I_{\text{corr}}/T)$  and  $1000/T$  at different temperatures.

**Table 4.** The value of activation parameters for carbon steel in 1.0 M HCl in the absence and presence of  $10^{-3}$  M of CTPTC.

Inhibitor	Linear regression coefficient (r)	$E_a$ (kJ/mol)	$\Delta H_a$ (kJ/mol)	$\Delta S_a$ (J/mol K)
Blank	0.905	52.28	49.64	-35.15
CTPTC	0.993	87.15	84.51	52.06

Inspection of these data revealed that the thermodynamic parameters ( $\Delta S_a$  and  $\Delta H_a$ ) for dissolution reaction of carbon steel in 1.0 M HCl in the presence of inhibitor are higher than that obtained in the absence of inhibitor. The positive sign of  $\Delta H_a$  reflects the endothermic nature of the carbon steel dissolution process suggesting that the dissolution of carbon steel is slow [54] in the presence of inhibitor. The large negative value of  $\Delta S_a$  for carbon steel in 1.0 M HCl implies that the activated complex is the rate-determining step, rather than the dissociation step. In the presence of the inhibitor, the value of  $\Delta S_a$  increases and is generally interpreted as an increase in disorder as the reactants are converted to the activated complexes [55].

### 3.3.3. Adsorption and thermodynamic considerations

The extent of corrosion inhibition depends on the surface conditions and the mode of adsorption of the inhibitors [56]. Under the assumptions that the corrosion of the covered parts of the surface is equal to zero and that corrosion takes place only on the uncovered parts of the surface (i.e., inhibitor efficiency is due mainly to the blocking effect of the adsorbed species), the degree of surface

coverage  $\theta$  has been estimated from the electrochemical impedance spectroscopy (EIS) technique employed in this study as follows:  $\theta = \eta_z\% / 100$  (assuming a direct relationship between surface coverage and inhibition efficiency) [56-59].

The adsorption on the corroding surfaces never reaches the real equilibrium and tends to reach an adsorption steady state. However, when the corrosion rate is sufficiently small, the adsorption steady state has a tendency to become a quasi-equilibrium state. In this case, it is reasonable to consider the quasi-equilibrium adsorption in thermodynamic way using the appropriate equilibrium adsorption isotherms [60].

Basic information on the interaction between the inhibitor and the carbon steel surface can be provided by the adsorption isotherm. In order to obtain the isotherm, the linear relation between the values of  $\theta$  and the inhibitor concentration ( $C_{inh}$ ) must be found. Attempts were made to fit the  $\theta$  values to various isotherms including Langmuir, Hill de Boer, Parsons, Temkin, Flory-Huggins, Dahar-Flory-Huggins and Bockris-Swinkel. By far the best fit is obtained with Langmuir isotherm. According to this isotherm,  $\theta$  is related to  $C_{inh}$  by:

$$\frac{C_{inh}}{\theta} = \frac{1}{K_{ads}} + C_{inh} \quad (12)$$

where  $K_{ads}$  is the adsorption constant,  $C_{inh}$  is the concentration of the inhibitor and surface coverage values ( $\theta$ ) are obtained from the EIS measurements for various concentrations.

Fig. 6 shows the relationship between  $C_{inh} / \theta$  and  $C_{inh}$  for the pyrimidothiazine derivative at 303 K. The correlation coefficient ( $R^2$ ) was used to choose the isotherm that best fit experimental data (Table 5). The linear correlation coefficient ( $R^2$ ) is equal to one. The slope of the straight line for this inhibitor was close to unity. Data illustrated in Fig. 6 indicated that the adsorption process obeyed Langmuir adsorption isotherm. Langmuir's isotherm assumes that there is no interaction between the adsorbed molecules, the energy of adsorption is independent on the surface coverage ( $\theta$ ), the solid surface contains a fixed number of adsorption sites, and each site holds one adsorbed species.

The equilibrium constant for adsorption process is related to the free energy of adsorption,  $\Delta G_{ads}^\circ$ , and is expressed by following equation:

$$K_{ads} = \left(\frac{1}{55.5}\right) \exp\left(-\frac{\Delta G_{ads}^\circ}{RT}\right) \quad (13)$$

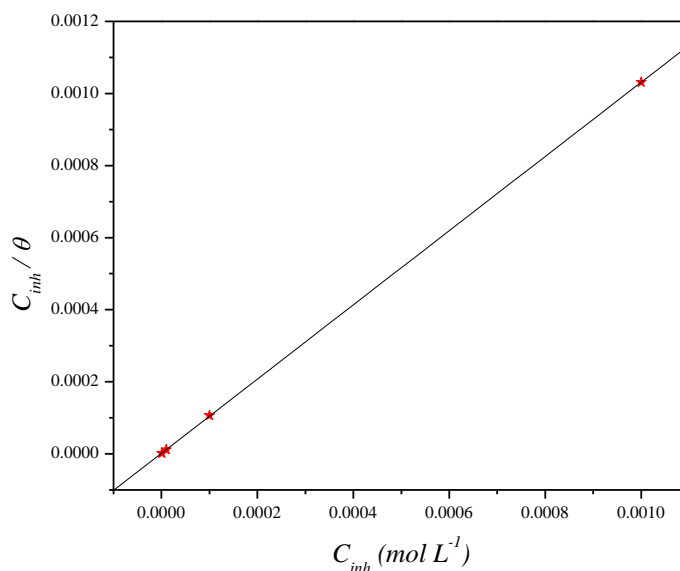
where  $R$  is gas constant and  $T$  is absolute temperature of experiment and the constant value of 55.5 is the concentration of water in solution in  $\text{mol L}^{-1}$ .

The thermodynamics parameters derived from Langmuir adsorption isotherm for the studied compound, are given in Table 5. The negative value of  $\Delta G_{ads}^\circ$  along with the high  $K_{ads}$  indicate a spontaneous adsorption process [61].

**Table 5.** Thermodynamic parameters for the adsorption of CHPPC in 1.0 M HCl on the carbon steel at 303 K.

Inhibitor	Slope	$K_{ads}$ ( $M^{-1}$ )	$R^2$	$\Delta G_{ads}^\circ$ (kJ/mol)
CHPPC	1.03	608220.71	1.0	-43.67

Generally, the energy values of  $-20 \text{ kJ mol}^{-1}$  or less negative are associated with an electrostatic interaction between charged molecules and charged metal surface, physisorption; those of  $-40 \text{ kJ mol}^{-1}$  or more negative involve charge sharing or transfer from the inhibitor molecules to the metal surface to form a coordinate covalent bond, chemisorption [62,63]. The value of  $\Delta G_{ads}^\circ$  is equal to  $-43.67 \text{ kJ mol}^{-1}$ . The large value of  $\Delta G_{ads}^\circ$  and its negative sign is usually characteristic of strong interaction and a highly efficient adsorption [64]. The high value of  $\Delta G_{ads}^\circ$  shows that in the presence of 1.0 M HCl chemisorption of CHPPC may occur. The possible mechanisms for chemisorption can be attributed to the donation of  $\pi$ -electron in the aromatic rings, the presence of three nitrogen, three oxygen and one sulfur atom in inhibitor molecule as reactive centers is an electrostatic adsorption of the protonated pyrimidothiazine derivative compound in acidic solution to adsorb on the metal surface.

**Figure 6.** Langmuir adsorption of CHPPC on the carbon steel surface in 1.0 HCl solution.

### 3.3. Quantum Chemical Calculations

The structure and electronic parameters were obtained by means of theoretical calculations using the computational methodologies of quantum chemistry. The optimized molecular structures and frontier molecular orbital density distribution of the studied molecule are shown in Figure 7. The

calculated quantum chemical parameters such as  $E_{\text{HOMO}}$ ,  $E_{\text{LUMO}}$ ,  $\Delta E_{\text{LUMO-HOMO}}$ , dipole moment ( $\mu$ ) and  $\Delta N$  are listed in Table 6.

**Table 6.** Calculated quantum chemical parameters of CHPPC.

Quantum Parameters	CHPPC
$E_{\text{HOMO}}$ (eV)	-7.6977
$E_{\text{LUMO}}$ (eV)	- 5.9320
$\Delta E_{\text{LUMO-HOMO}}$ (eV)	1.7657
dipole moment ( $\mu$ ) (Debye)	12.1039
$\Delta N$ (eV)	0.05242963

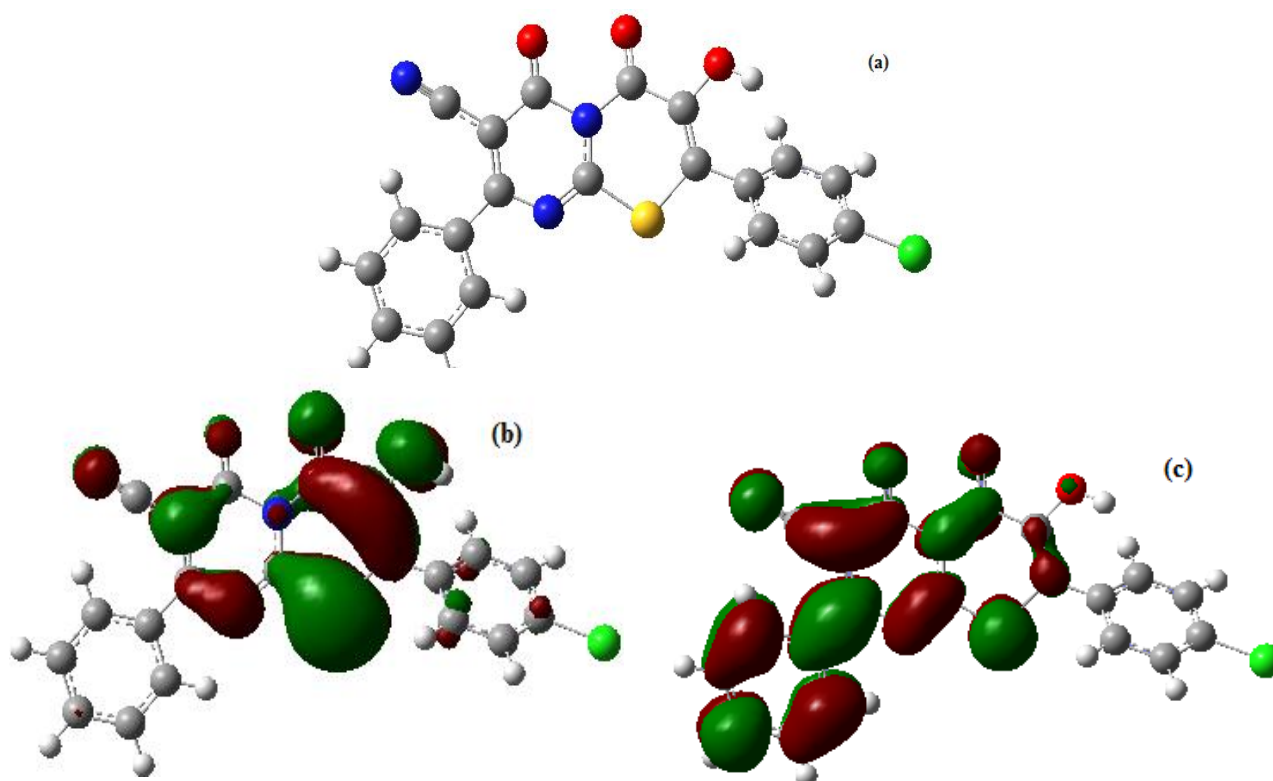


**Figure 7.** (a) Optimized molecular structure (b) HOMO and (c) LUMO molecular orbital density distribution of CHPPC.

The value of highest occupied molecular orbital,  $E_{\text{HOMO}}$  indicates the tendency of the molecule to donate electrons to acceptor molecule with empty and low energy orbital. Therefore, the energy of the lowest unoccupied molecular orbital,  $E_{\text{LUMO}}$  indicates the tendency of the molecule to accept electrons [65]. The energy gap  $\Delta E$  is an important parameter which is related to reactivity of the inhibitor molecule towards the metal surface. The interaction of inhibitor molecule to the metal surface is related to transfer of electrons from inhibitor to metal surface [66].

The fraction of electrons transferred from inhibitor to the iron molecule ( $\Delta N$ ) was calculated. According to other reports [34,67], value of  $\Delta N$  showed inhibition effect resulted from electron

donation. In this study, the CHPPC was the donators of electrons while the carbon steel surface was the acceptor. The CHPPC was bound to the carbon steel surface, and thus formed inhibition adsorption layer against corrosion.

#### 4. CONCLUSION

CHPPC acts as an excellent mixed type inhibitor with predominant cathodic action for the corrosion of carbon steel in 1.0 M HCl solution. Inhibition efficiency increases with increase in concentration of Ind1 but decreases with rise temperature. The surface adsorption of the used inhibitor led to a reduction in the double layer capacitance as well as an increase in the charge transfer resistance. The adsorption of CHPPC follows Langmuir adsorption isotherm. Inhibitive action is due to chemical adsorption of CHPPC on carbon steel surface and the adsorption process is a spontaneous and exothermic process.

#### ACKNOWLEDGEMENTS

Prof S. S. Al-Deyab and Prof B. Hammouti extend their appreciation to the Deanship of Scientific Research at king Saud University for funding the work through the research group project.

#### References

1. S.A. Umoren, O. Ogbobe, I.O. Igwes, E.E. Ebenso, *Corros. Sci.* 50 (2008) 1998
2. A. Zarrouk, B. Hammouti, H. Zarrok, R. Salghi, A. Dafali, Lh. Bazzi, L. Bammou, S. S. Al-Deyab, *Der Pharm. Chem.* 4 (2012) 337.
3. H. Zarrok, R. Saddik, H. Oudda, B. Hammouti, A. El Midaoui, A. Zarrouk, N. Benchat, M. Ebn Touhami, *Der Pharm. Chem.* 3 (2011) 272.
4. D. Ben Hmamou, R. Salghi, A. Zarrouk, B. Hammouti, S.S. Al-Deyab, Lh. Bazzi, H. Zarrok, A. Chakir, L. Bammou, *Int. J. Electrochem. Sci.* 7 (2012) 2361.
5. A. Zarrouk, B. Hammouti, A. Dafali, H. Zarrok, *Der Pharm. Chem.* 3 (2011) 266.
6. A. Ghazoui, R. Saddik, N. Benchat, B. Hammouti, M. Guenbour, A. Zarrouk, M. Ramdani, *Der Pharm. Chem.* 4 (2012) 352.
7. A. Zarrouk, B. Hammouti, H. Zarrok, I. Warad, M. Bouachrine, *Der Pharm. Chem.* 3 (2011) 263.
8. D. Ben Hmamou, R. Salghi, A. Zarrouk, M. Messali, H. Zarrok, M. Errami, B. Hammouti, Lh. Bazzi, A. Chakir, *Der Pharm. Chem.* 4 (2012) 1496.
9. H. Bendaha, A. Zarrouk, A. Aouniti, B. Hammouti, S. El Kadiri, R. Salghi, R. Touzani, *Phys. Chem. News*, 64 (2012) 95.
10. S. Rekkab, H. Zarrok, R. Salghi, A. Zarrouk, Lh. Bazzi, B. Hammouti, Z. Kabouche, R. Touzani, M. Zougagh, *J. Mater. Environ. Sci.* 3 (2012) 613.
11. H. Zarrok, A. Zarrouk, R. Salghi, Y. Ramli, B. Hammouti, M. Assouag, E. M. Essassi, H. Oudda and M. Taleb, *J. Chem. Pharm. Res.* 4 (2012) 5048.
12. H. Zarrok, H. Oudda, A. El Midaoui, A. Zarrouk, B. Hammouti, M. Ebn Touhami, A. Attayibat, S. Radi, R. Touzani, *Res. Chem. Intermed.* 38 (2012) 2051.
13. A. Ghazoui, A. Zarrouk, N. Bencat, R. Salghi, M. Assouag, M. El Hezzat, A. Guenbour, B. Hammouti, *J. Chem. Pharm. Res.* 6 (2014) 704.
14. A. Zarrouk, H. Zarrok, R. Salghi, R. Tour, B. Hammouti, N. Benchat, L. Afrine, H. Hannache, M. El Hezzat, M. Bouachrine, *J. Chem. Pharm. Res.* 5 (2013) 1482.

15. D. Ben Hmamou, M. R. Aouad, R. Salghi, A. Zarrouk, M. Assouag, O. Benali, M. Messali, H. Zarrouk, B. Hammouti, *J. Chem. Pharm. Res.* 4 (2012) 3489.
16. L. Afrine, A. Zarrouk, H. Zarrouk, R. Salghi, R. Tourir, B. Hammouti, H. Oudda, M. Assouag, H. Hannache, M. El Harti, M. Bouachrine, *J. Chem. Pharm. Res.* 5 (2013) 1474.
17. A. Zarrouk, B. Hammouti, A. Dafali, F. Bentiss, *Ind. Eng. Chem. Res.* (2013) 2560.
18. H. Zarrouk, A. Zarrouk, R. Salghi, H. Oudda, B. Hammouti, M. EbnTouhami, M. Bouachrine, O.H. Pucci, *Port. Electrochim. Acta*, 30 (2012) 405.
19. A. Zarrouk, B. Hammouti, H. Zarrouk, S.S. Al-Deyab, S.S., I. Warad, *Res. Chem. Intermed.* 38 (2012) 1655.
20. H. Zarrouk, A. Zarrouk, R. Salghi, B. Hammouti, M. Elbakri, M. Ebn touhami, F. Bentiss, H. Oudda, *Res. Chem. Intermed.* 40 (2014) 801.
21. A. Zarrouk, B. Hammouti, T. Lakhlifi, M. Traisnel, H. Vezin, F. Bentiss, *Corros. Sci.* 90 (2015) 572.
22. Y. ELaoufir, H. Bourazmi, H. Serrar, H. Zarrouk, A. Zarrouk, B. Hammouti, A. Guenbour, S. Boukhriss, H. Oudda, *Der Pharma. Lett.* 6 (2014) 526.
23. I.L. Rozendeld, *Corrosion Inhibitors*, McGraw-Hill, New York, NY, 1981.
24. S.K. Rangarajan, *J. Electroanal. Chem.* 82 (1977) 93.
25. H. Ma, S. Chen, Z. Liu, Y. Sun, *J. Mol. Struct. (THEOCHEM)* 774 (2006) 1922.
26. J.H. Henrquez-Romn, L. Padilla-Campos, M.A. Pez, J.H. Zagal, M.A. Rubio, C.M. Rangel, J. Costamagna, G. Crdenas-Jirn, *J. Mol. Struct. (THEOCHEM)* 757 (2005) 17.
27. L.M. Rodriguez-Valdez, A. Martinez-Villafane, D. Glossman-Mitnik, *J. Mol. Struct. (THEOCHEM)* 713 (2005) 6570.
28. Y. Feng, S. Chen, W. Guo, Y. Zhang, G. Liu, *J. Electroanal. Chem.*, **2007**, 602, 115122.
29. M. J. Frisch, G. W. Trucks, H. B. Schlegel, G. E. Scuseria, M. A. Robb, J. R. Cheeseman, J. A. Montgomery, Jr., T. Vreven, K. N. Kudin, J. C. Burant, J. M. Millam, S. S. Iyengar, J. Tomasi, V. Barone, B. Mennucci, M. Cossi, G. Scalmani, N. Rega, G. A. Petersson, H. Nakatsuji, M. Hada, M. Ehara, K. Toyota, R. Fukuda, J. Hasegawa, M. Ishida, T. Nakajima, Y. Honda, O. Kitao, H. Nakai, M. Klene, X. Li, J. E. Knox, H. P. Hratchian, J. B. Cross, V. Bakken, C. Adamo, J. Jaramillo, R. Gomperts, R. E. Stratmann, O. Yazyev, A. J. Austin, R. Cammi, C. Pomelli, J. W. Ochterski, P. Y. Ayala, K. Morokuma, G. A. Voth, P. Salvador, J. J. Dannenberg, V. G. Zakrzewski, S. Dapprich, A. D. Daniels, M. C. Strain, O. Farkas, D. K. Malick, A. D. Rabuck, K. Raghavachari, J. B. Foresman, J. V. Ortiz, Q. Cui, A. G. Baboul, S. Clifford, J. Cioslowski, B. B. Stefanov, G. Liu, A. Liashenko, P. Piskorz, I. Komaromi, R. L. Martin, D. J. Fox, T. Keith, M. A. Al-Laham, C. Y. Peng, A. Nanayakkara, M. Challacombe, P. M. W. Gill, B. Johnson, W. Chen, M. W. Wong, C. Gonzalez, and J. A. Pople, *Gaussian 03, Revision E.01*, Gaussian, Inc., Wallingford CT, 2004.
30. M.J.S. Dewar, W. Thiel, *J. Am. Chem. Soc.* 99 (1977) 4899.
31. R.G. Pearson, *Inorg. Chem.* 27 (1988) 734.
32. V.S. Sastri, J.R. Perumareddi, *Corrosion (NACE)* 53 (1997) 617.
33. I. Lukovits, E. Kalman, F. Zucchi, *Corrosion (NACE)* 57 (2001) 3.
34. S. Xia, M. Qui, L. Yu, F. Lui, *Corros. Sci.* 50 (2008) 2021.
35. G.N. Mu, X.H. Li, Q. Qu, J. Zhou, *Corros. Sci.* 48 (2006) 445.
36. X. Li, S. Deng, H. Fu, T. Li, *Electrochim. Acta*, 54 (2009) 89.
37. M. Bouklah, N. Benchat, B. Hammouti, A. Aouniti, S. Kertit, *Mater. Lett.* 60 (2005) 1901.
38. S. S. Abd El Rehim, H. H. Hassan, M. A. Amin, *Mater. Chem. Phys.* 78 (2002) 337.
39. Q. Zhang, Y. Hua, *Mater. Chem. Phys.* 119 (2010) 57.
40. K. F. Khaled, *Corros. Sci.* 52 (2010) 2905.
41. H. Amar, T. Braisaz, D. Villemin, B. Moreau, *Mater. Chem. Phys.* 110 (2008) 1.
42. A. H. Mehaute, G. Grep, *Solid State Ionics*, 910 (1989) 17.
43. R. Solmaz, E. Altunbas, G. Kardas, *Mater. Chem. Phys.* 125 (2011) 796.

44. A. Chetouani, A. Aouniti, B. Hammouti, N. Benchat, T. Benhadda, S. Kertit, *Corros. Sci.* 45 (2003) 1675.
45. M. Behpour, S. M. Ghoreishi, N. Soltani, M. Salavati-Niasari, *Corros. Sci.* 51 (2009) 1073.
46. M. Hosseini, S. Mertens, M. Ghorbani, *Mater. Chem. Phys.* 78 (2003) 800.
47. E. Kus, F. Mansfeld, *Corros. Sci.* 48 (2006) 965.
48. F. Beck, U.A. Kruger, *Electrochim. Acta* 41(1996) 1083.
49. P. W. Atkins, *Physical Chemistry*, 5<sup>th</sup> ed., University Press, Oxford, 1994, P. 877.
50. R. Sanchez-Tovar, M.T. Montanes, J. Garcia-Anton, *Corros. Sci.* 52 (2010) 722.
51. S. Martinez, I. Stern, *Appl. Surf. Sci.*, 199 (2002) 83.
52. A.A. Khadom, A.S. Yaro, A.A.H. Kadhum, A.S. Al Taie, A.Y. Musa, *J. Appl. Sci.* 6 (2009) 1403.
53. N.M. Guan, L. Xueming, L. Fei, *Mater. Chem. Phys.* 86 (2004) 59.
54. S.M.A. Hosseini, M. Salari, M. Ghasemi, M. Abaszadeh, *Z. Phys. Chem.* 223 (2009) 769.
55. M. Christov, A. Popova, *Corros. Sci.* 46 (2004) 1613.
56. B.B. Damaskin, O.A. Petrii, B. Batrakov, *Adsorption of Organic Compounds on Electrodes*, Plenum Press, New York, 1971.
57. I. Langmuir, *J. Am. Chem. Soc.* 39 (1917) 1848.
58. R. Alberty, R. Silbey, *Physical Chemistry*, second ed., Wiley, New York, 1997. p. 845.
59. I.D. Mall, V.C. Srivastava, N.K. Agrwal, I.M. Mishra, *Colloids Surf. A: Physicochem. Eng. Aspects* 264 (2005) 17.
60. M. Scendo, *Corros. Sci.* 49 (2007) 373.
61. F.M. Donahue, K. Nobe, *J. Electrochem. Soc.* 112 (1965) 886.
62. E. Kamis, F. Bellucci, R.M. Latanision, E.S.H. El-Ashry, *Corrosion* 47 (1991) 677.
63. M. Abdallah, *Corros. Sci.* 44 (2002) 717.
64. D. K. Yadav, M. A. Quraishi, *Ind. Eng. Chem. Res.* 51 (2012) 8194.
65. N. Khalil, *Electrochim. Acta*, 48 (2003) 2635.
66. H. Ju, Z. Kai, Y. Li, *Corros. Sci.* 50 (2008) 865.